SUPPLEMENTARY ONLINE MATERIAL

Title: KCNQ4 K+ channels tune mechanoreceptors for normal touch sensation in mouse and man

Authors: Matthias Heidenreich*, Stefan G. Lechner*, Vitya Vardanyan, Christiane Wetzel, Cor W. Cremers, Els M. De Leenheer, Gracia Aránguez, Miguel Ángel Moreno-Pelayo, Thomas J. Jentsch, Gary R. Lewin

Nature Neuroscience doi:10.1038/nn.2985

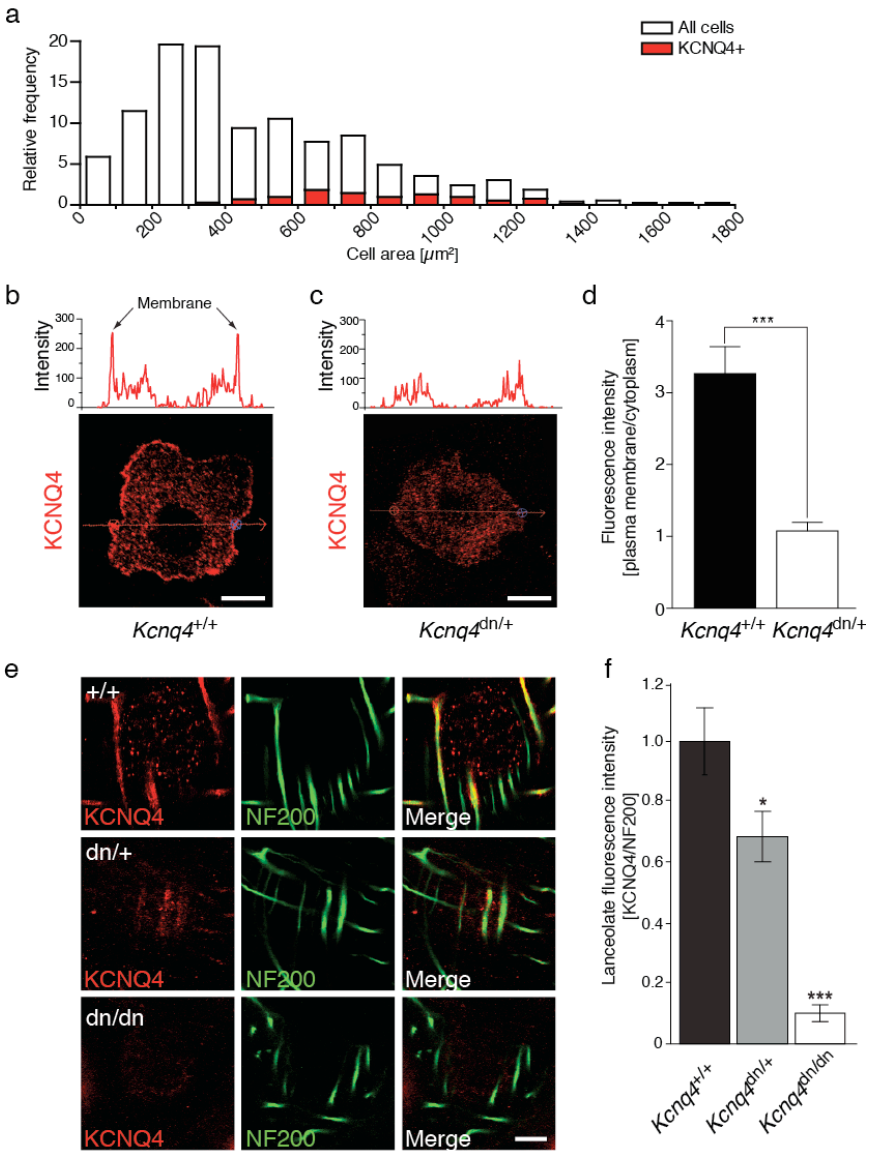

Supplementary Figure 1 Immunohistochemical analysis of KCNQ4 expression in mouse DRGs and skin. (**a**) Correlation between cell size and KCNQ4 expression. KCNQ4-expressing DRG neurons have medium to large somata. (**b**) Line scan analysis of WT DRG neurons labeled for KCNQ4 (antibody rbKCNQ4KC) demonstrates partial plasma membrane localization of KCNQ4. The arrow indicates the measured fluorescence intensity over the DRG neuron as shown below. KCNQ4 is also present in intracellular vesicular structures of unknown identity, as evident from the punctuate staining of the cytoplasm. (**c**) Line scan analysis of *Kcnq4*$^{dn/+}$ DRG neurons demonstrates loss of plasma membrane localization of KCNQ4 in *Kcnq4*$^{dn/+}$ neurons compared to *Kcnq4*$^{+/+}$. The arrow indicates the direction of the scan, with intensity being displayed below. (**d**) Quantification of line scan analysis demonstrates a significant reduction of plasma membrane to cytoplasm fluorescence intensity ratio of KCNQ4 in *Kcnq4*$^{dn/+}$ DRG neurons compared to *Kcnq4*$^{+/+}$ neurons (n=16 neurons/genotype from 3 different animals/genotype, ***, $P < 0.001$, Student´s *t*-test). (**e**) Confocal images of lanceolate nerve endings of *Kcnq4*$^{+/+}$, *Kcnq4*$^{dn/+}$ and *Kcnq4*$^{dn/dn}$ mice. Sections were stained for KCNQ4 (antibody rbKCNQ4KC) and NF200 and quantified. (**f**) Quantification of KCNQ4 in NF200 stained follicular fiber networks of *Kcnq4*$^{+/+}$, *Kcnq4*$^{dn/+}$ and *Kcnq4*$^{dn/dn}$ mice. KCNQ4 labeling was significantly reduced in lanceolate endings from *Kcnq4*$^{dn/+}$ (*, $P < 0.05$, Student`s *t*-test) mice and was nearly absent in hair follicles from *Kcnq4*$^{dn/dn}$ mice (***, $P < 0.001$, Student`s *t*-test) compared to *Kcnq4*$^{+/+}$ mice (n=20 from 3 mice/genotype). Scale bars: 10 µm. Error bars are s.e.m.

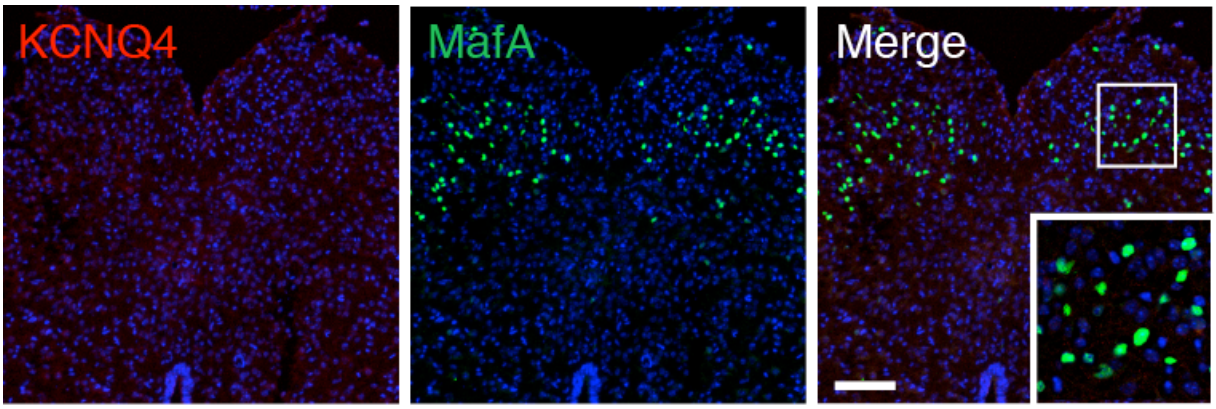

Supplementary Figure 2 KCNQ4 is not expressed in MafA positive neurons of the spinal cord. KCNQ4 is not expressed in the dorsal spinal cord, although there is a population of MafA-positive cells. Inset shows a higher magnification. Nuclei were labeled with DAPI (blue). Scale bar: 200 μm.

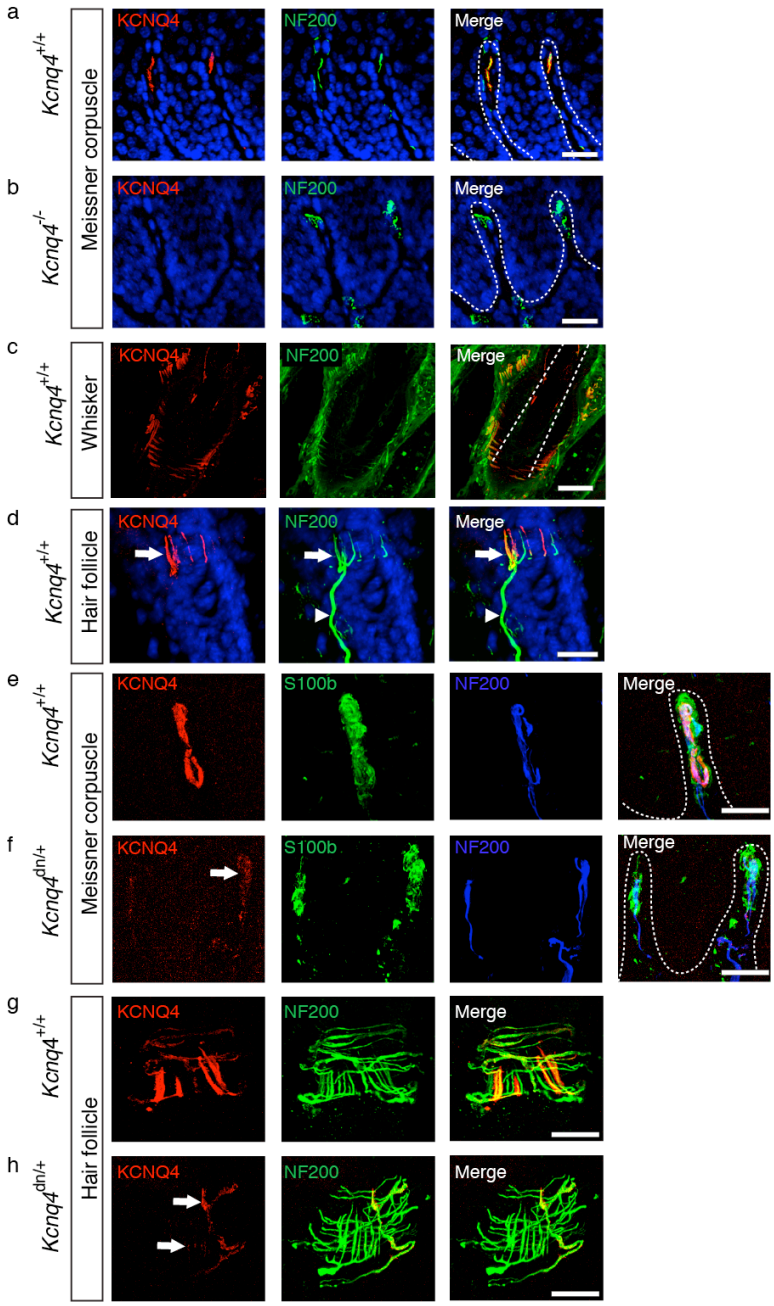

Supplementary Figure 3 Localization of KCNQ4 in mouse glabrous, hairy skin and whiskers. Skin sections were labeled with antibodies against KCNQ4 (antibody gpKCNQ4A), NF200 and S100b. Nuclei were visualized with DAPI (blue) in (**a**), (**b**) and (**d**). (**a**) KCNQ4 co-localizes with NF200 in Meissner corpuscles (dotted line) of WT mice, but is absent from Meissner corpuscles (dotted line) of *Kcnq4*$^{-/-}$ mice (**b**). No morphological abnormalities are observed. (**c**) Immunofluorescence analysis of a mouse whisker hair follicle shows KCNQ4 staining of NF200-positive nerve endings in the follicular fiber network. Dotted lines indicate borders of hair shaft.. (**d**) Expression of KCNQ4 is restricted to NF200-positive lanceolate endings (arrow) and does not extend proximally to the afferent stem axon (arrowhead). (**e**,**f**) Meissner corpuscles from *Kcnq4*$^{+/+}$ and *Kcnq4*$^{dn/+}$ mice were triple labeled with antibodies against KCNQ4, S100b and NF200. KCNQ4 is expressed at the nerve endings within Meissner corpuscles (dotted line) in WT mice (e). KCNQ4 expression is reduced in Meissner corpuscles (dotted line) of *Kcnq4*$^{dn/+}$ mice (f, arrow). No morphological abnormalities are observed. (**g**) KCNQ4 labeling of lanceolate and circular nerve endings. (**h**) KCNQ4 labeling of lanceolate and circular nerve endings is reduced in *Kcnq4*$^{dn/+}$ mice (arrows). No morphological abnormalities are observed. Scale bars: 20 µm (**a**-**d**), 25 µm (**e**-**h**).

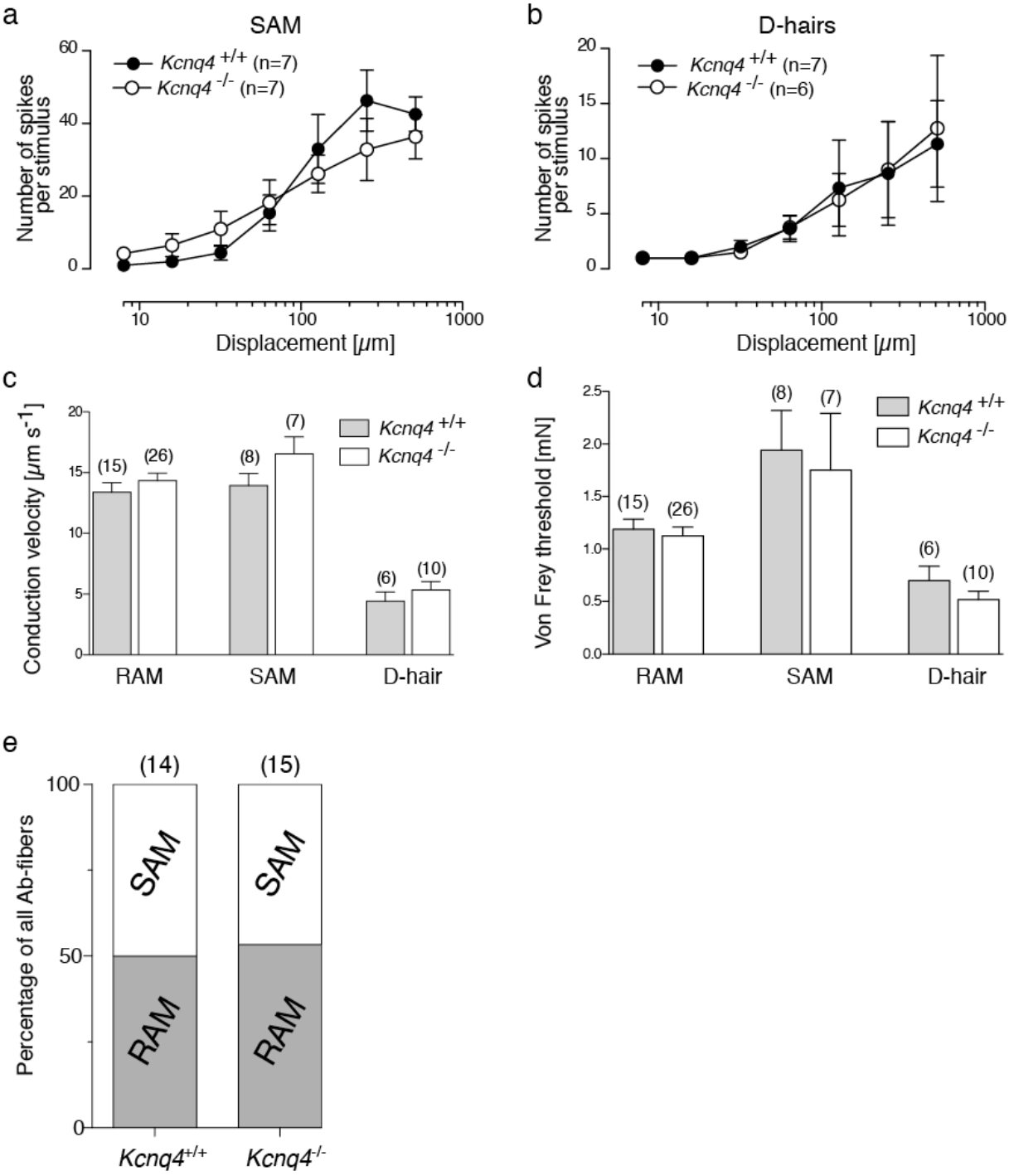

Supplementary Figure 4 Lack of KCNQ4 does not affect firing properties of SAMs and D-hairs. (**a**,**b**) Receptive fields of SAMs (**a**) and D-hairs (**b**) were stimulated with mechanical ramp-and-hold stimuli of increasing amplitudes, but constant ramp velocities. (**c**,**d**) Single units were classified according to their conduction velocity (CV (**c**)), (A-beta fibers (RAMs and SAMs) CV > 10 m/s; thinly myelinated A-delta fibers (D-hairs) CV = 1-10 m/s)), von Frey thresholds (VFT (**d**)) and their adaptation properties to supra-threshold stimulation[1]; Neither CV (**c**) nor VFT (**d**) was changed in the absence of KCNQ4. (**e**) Quantitative comparison of the proportions of RAMs and SAMs present in *Kcnq4*$^{+/+}$ and *Kcnq4*$^{-/-}$ mice. Data from three mice per genotype is shown. No significant differences were observed. All error bars represent s.e.m.

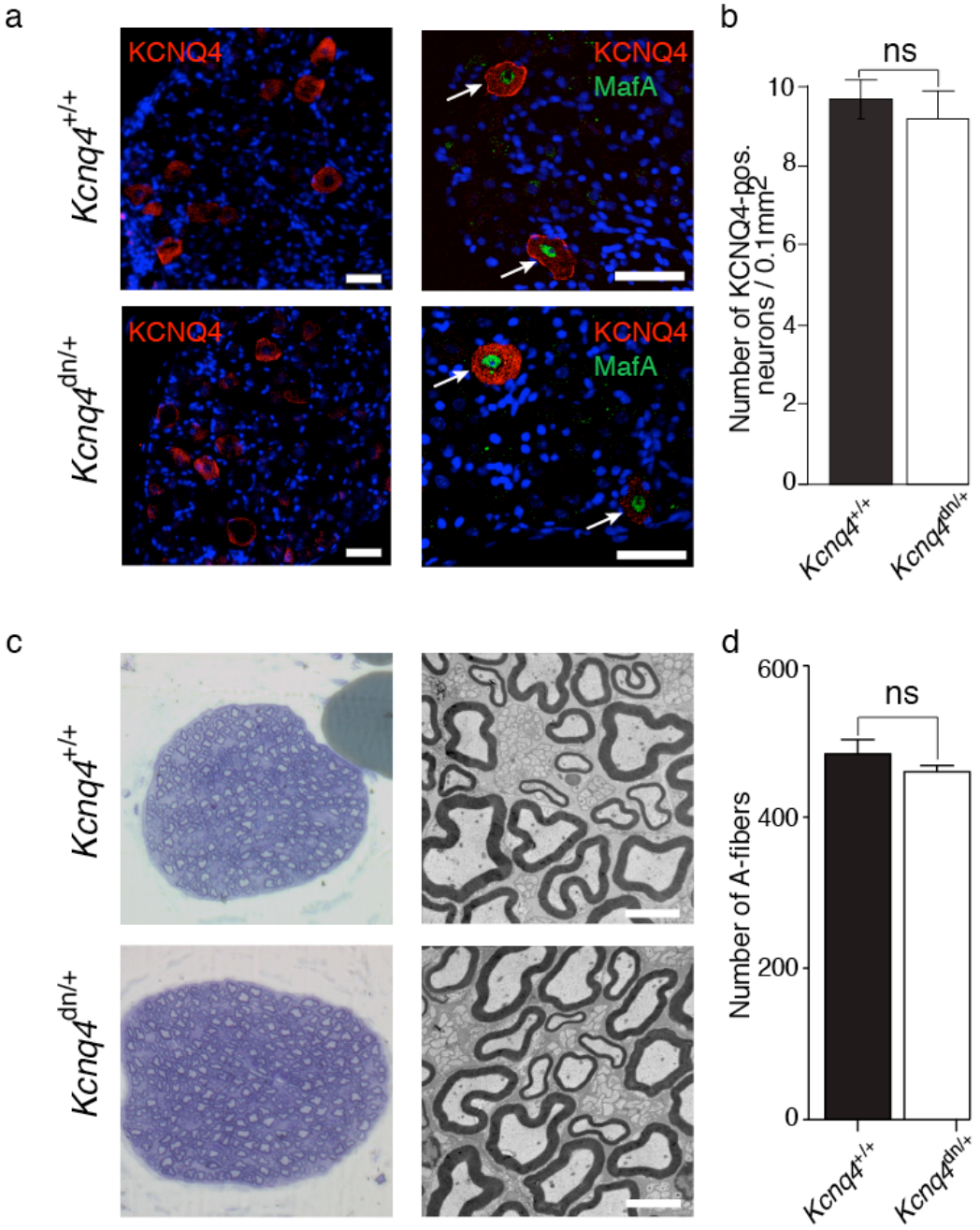

Supplementary Figure 5 No evidence for neuronal degeneration in KCNQ4 mutant mice. (**a,b**) Quantitative comparison of KCNQ4 expressing DRG neurons of *Kcnq4*$^{+/+}$ and *Kcnq4*$^{dn/+}$ mice (left panel in a). Note, KCNQ4-positive neurons also express MafA (see also **Fig. 1e**) and MafA positive neurons were present in KCNQ4-mutant mice (right panel in a). Scale bars: 50µm. (**b**) KCNQ4-positive neurons were present in similar numbers in both genotypes (*P*=0.59, Student's *t*-test). (**c**) Electron micrographs of semithin (left panel) and ultrathin (70 nm, right panel, scale bar 2 µm) sections of the saphenous nerve from *Kcnq4*$^{+/+}$ (top) and *Kcnq4*$^{dn/+}$ (bottom) mice. (**d**) Comparison of the number of A-fibers. For each genotype the number of myelinated fibers from four semithin sections was quantified. No significant differences were observed when comparing fiber counts from *Kcnq4*$^{+/+}$ and *Kcnq4*$^{dn/+}$ mice (*P*=0.32, Student's *t*-test).

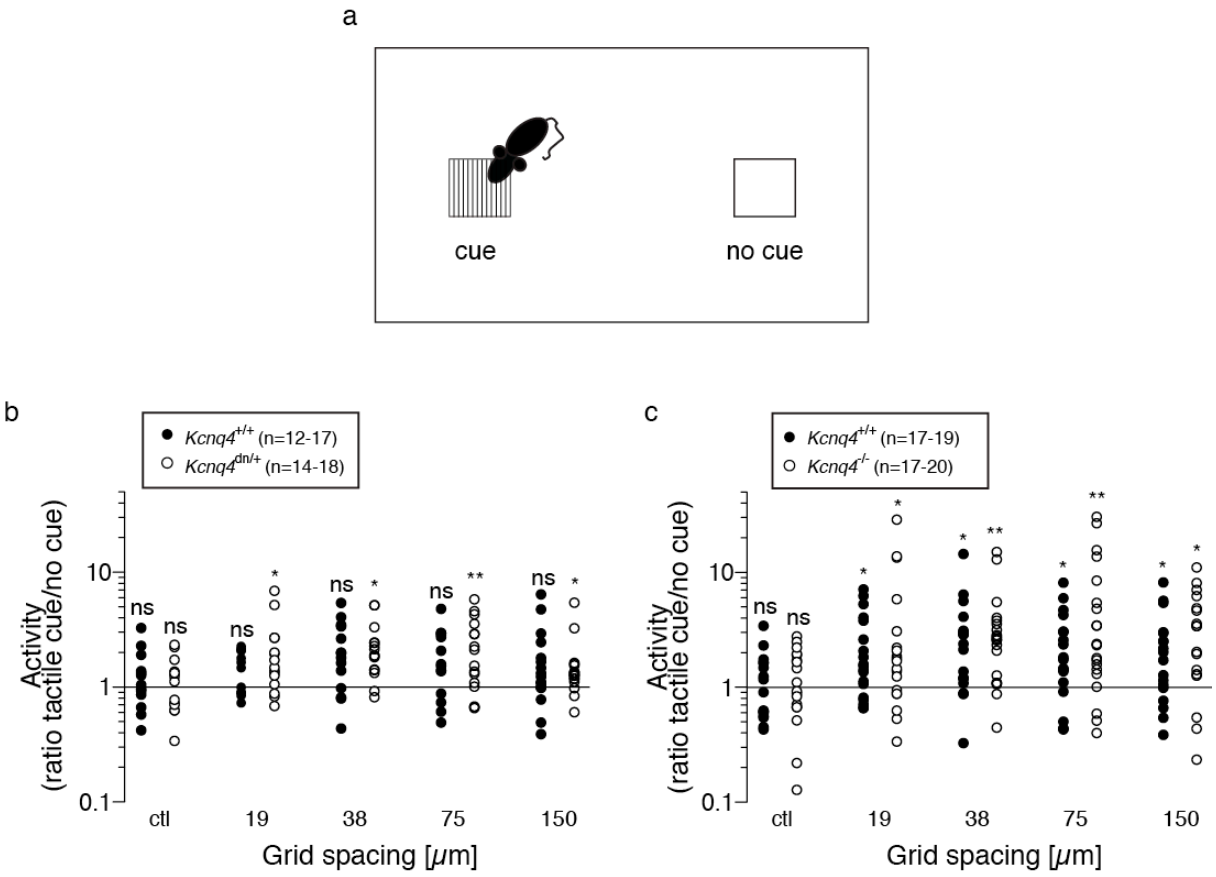

Supplementary Figure 6 Tactile-driven behavior of KCNQ4 mutant mice. (**a**) Schematic drawing of experimental arrangement. The grid (cue) is placed in one of two spatially equivalent positions. The control area is labeled as `no cue´. To determine whether mice recognize a grid of a certain size, the time spent actively exploring the grid was compared to the time spent exploring an equally sized and located control area (no cue) with a smooth surface. Two blank areas placed in spatially equivalent positions were used as controls (ctl). Ratios larger than 1.0 indicate that mice are more active on the grid; ratios smaller than 1.0 indicate mice are less active on the grid. (**b**) Behavior of *Kcnq4*$^{+/+}$ (black circles) and *Kcnq4*$^{dn/+}$ (white circles) mice in mixed CBA/J and C57Bl/6J genetic background. *Kcnq4*$^{dn/+}$ mice spend significantly more time on the grid than on the control areas, whereas this ratio is not significantly different from 1 in age-matched *Kcnq4*$^{+/+}$ mice in exactly the same genetic background. While this suggests that *Kcnq4*$^{dn/+}$ mice recognize the grid better than WT control, directly comparing *Kcnq4*$^{+/+}$ and *Kcnq4*$^{dn/+}$ mice yields no significant difference. (**c**) Tactile-driven behavior of *Kcnq4*$^{+/+}$ (black circles) and *Kcnq4*$^{-/-}$ (white circles) mice in an inbred CH3 genetic background. Mice of both genotypes spent statistically significant more time on the grid than on the smooth control area. (*, $P < 0.05$, **, $P < 0.01$, Students`s paired *t*-test).

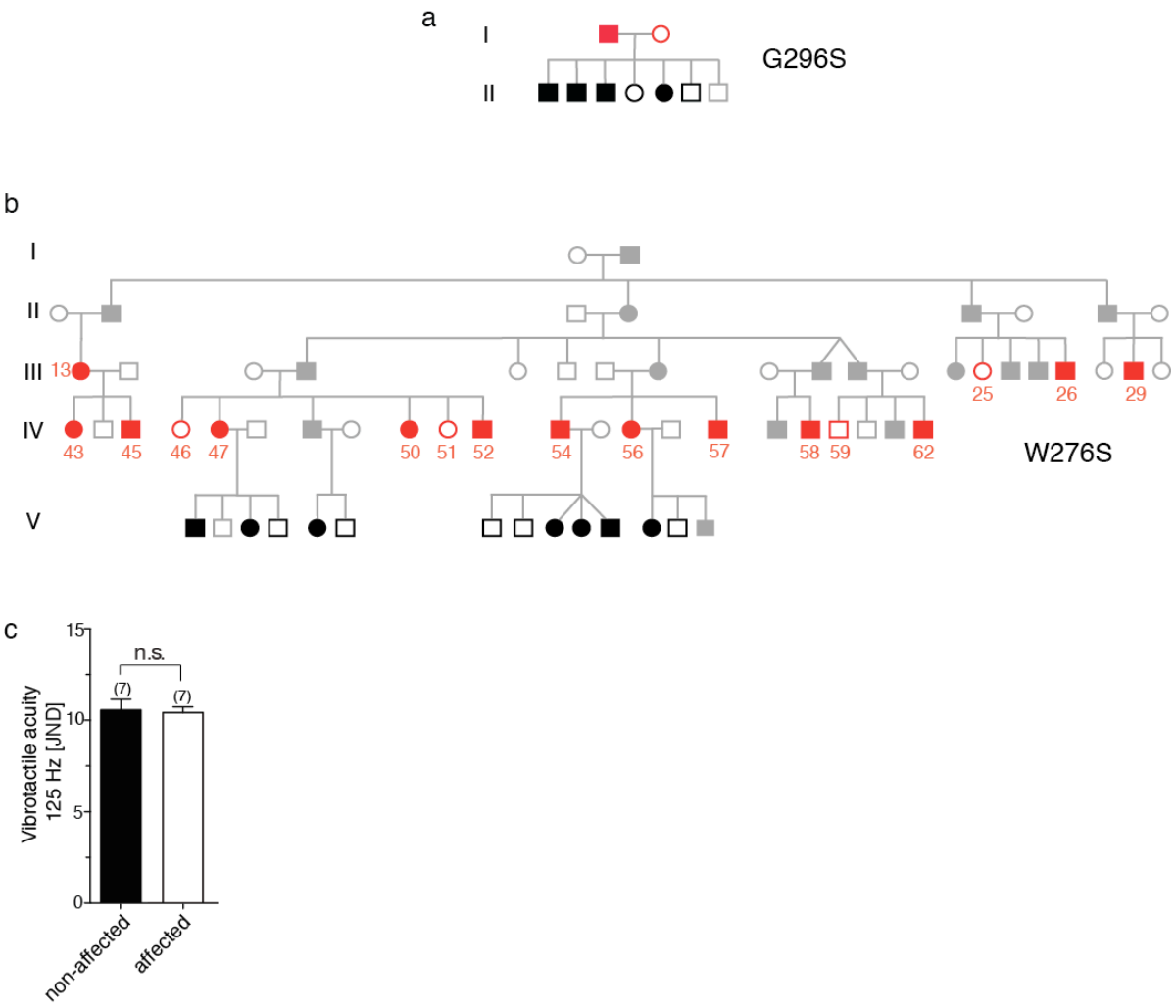

Supplementary Figure 7 Vibrotactile acuity of patients with DFNA2. (**a**,**b**) Pedigrees of the two studied DFNA2 cohorts previously identified by Mencia *et al.*[2] (**a**) and by De Leenheer *et al.*[3] (**b**). Women are depicted as circles and men as squares. Filled symbols indicate patients with DFNA2. Numbers are the same as used by De Leenheer and colleagues. Subjects that participated in this study are highlighted in red (age 37y - 55y) and black (age 14–23y), respectively. Due to large age-dependent inter-individual variations, children were excluded from the analysis. (**c**) Vibrotactile acuity of adult subjects (37-55 years) at 125 Hz as determined using a two-interval forced-choice vibrotactile acuity test (CaseIV; WR Medical Electronics). No significant differences were observed (JND, just noticeable difference). Error bars are s.e.m.

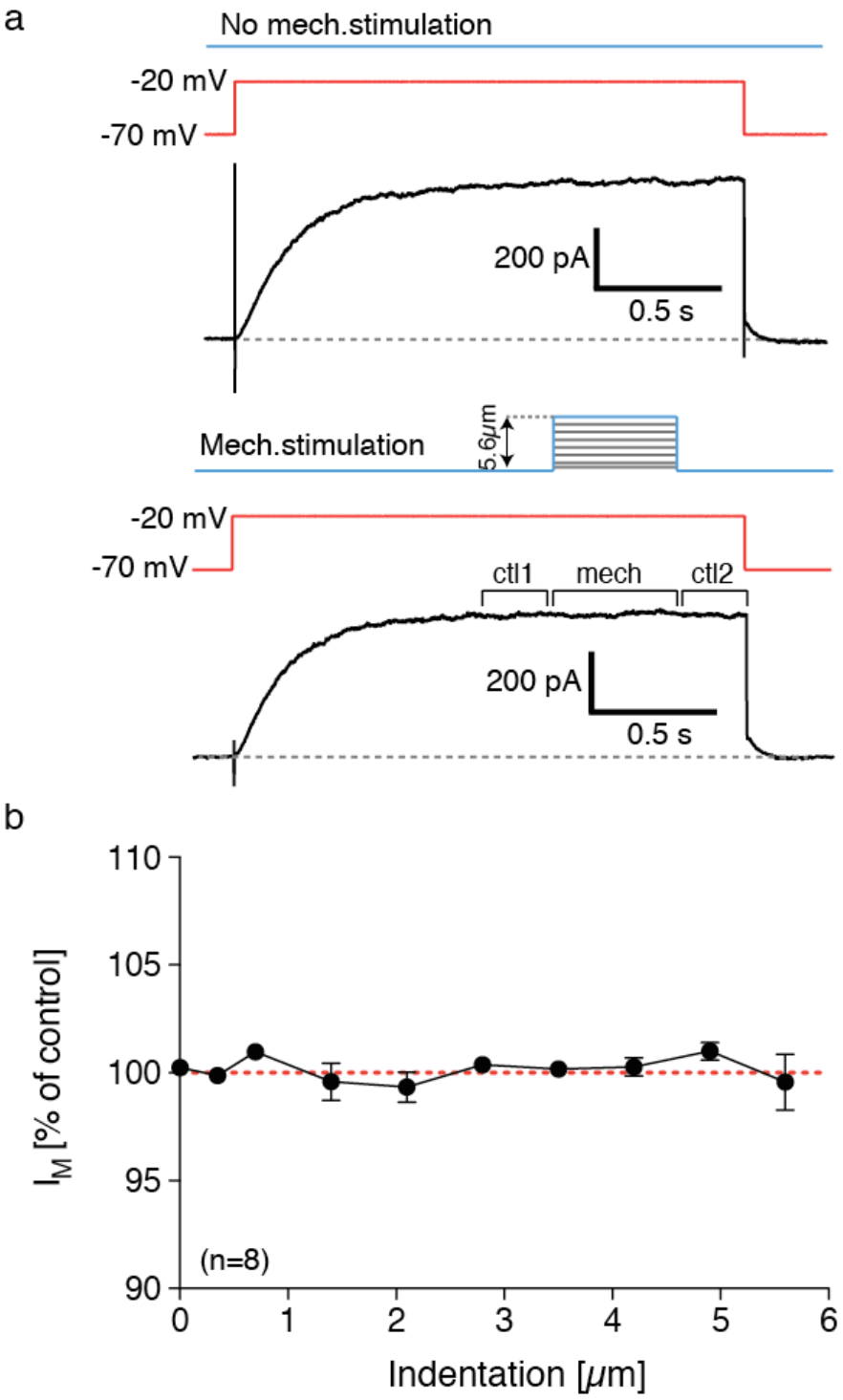

Supplementary Figure 8 Mechanical stimulation of KCNQ4 expressing HEK293 cells. (**a**) KCNQ4 mediated M-currents were activated every 20 seconds with step depolarizations from -70 mV to -20 mV (2 s duration, red trace). To test whether M-currents are sensitive to mechanical stimulation, cell membranes were indented with mechanical stimuli of increasing magnitude (blue trace, 350 nm to 5.6 µm), which were applied during steady state activation of KCNQ4. (**b**) M-current amplitudes during mechanical stimulation (mech, **a** bottom trace) were normalized to M-current amplitudes before (ctl1, **a** bottom trace) and after (ctl2, **a** bottom trace) mechanical stimulation (I_M[% of control] = 200*I_M^{mech}/(I_M^{ctl1}+I_M^{ctl2}) and plotted as a function of cell indentation. Note, M-current amplitudes did not change when mechanical force was applied to the cell membrane.

Nature Neuroscience doi:10.1038/nn.2985

Supplemental References

1. Koltzenburg, M., Stucky, C. & Lewin, G. Receptive properties of mouse sensory neurons innervating hairy skin. *J Neurophysiol* **78**, 1841-50 (1997).
2. Mencía, A. et al. A novel KCNQ4 pore-region mutation (p.G296S) causes deafness by impairing cell-surface channel expression. *Hum. Genet* **123**, 41-53 (2008).
3. De Leenheer, E.M.R. et al. Longitudinal and cross-sectional phenotype analysis in a new, large Dutch DFNA2/KCNQ4 family. *Ann. Otol. Rhinol. Laryngol* **111**, 267-274 (2002).